

## Circularly Polarized Laser Emission from an Electrically Pumped Chiral Microcavity

A.A. Maksimov<sup>1,\*</sup>, E.V. Filatov,<sup>1</sup> I. I. Tartakovskii,<sup>1</sup> V.D. Kulakovskii<sup>1</sup>, S.G. Tikhodeev,<sup>2,3</sup>  
C. Schneider,<sup>4</sup> and S. Höfling<sup>5</sup>

<sup>1</sup>Yu. A. Ossipyan Institute of Solid State Physics, Russian Academy of Sciences, Chernogolovka 142432, Russia

<sup>2</sup>M. V. Lomonosov Moscow State University, Leninskie Gory 1, Moscow 119991, Russia

<sup>3</sup>A. M. Prokhorov General Physical Institute, Russian Academy of Sciences, Vavilova Street 38, Moscow 119991, Russia

<sup>4</sup>Institute of Physics, University of Oldenburg, Oldenburg 26129, Germany

<sup>5</sup>Technische Physik and Wilhelm-Conrad-Röntgen-Research Center for Complex Material Systems, Universität Würzburg, Am Hubland, Würzburg 97074, Germany



(Received 10 September 2021; revised 7 December 2021; accepted 24 January 2022; published 10 February 2022)

Engineering the chirality of optical microcavities is a central concept of modern photonics to gain full control the polarization of the confined electromagnetic mode. Here, we demonstrate a compact source of coherent radiation based on an electrically driven, chiral semiconductor microcavity. The device is composed of an AlAs/(Al, Ga)As microcavity containing multiple GaAs quantum wells in the active region and a chiral photonic crystal slab etched in the upper distributed Bragg reflector. The structure promotes laser oscillation under electrical current injection in the near-infrared spectral range ( $\hbar\omega \simeq 1.565$  eV) and degrees of circular polarization exceeding 90%. The sense of circular polarization is controlled by the handedness of the chiral photonic crystal slab and changes to the opposite one in a mirror-symmetrical structure. Our results represent an important step towards the practical implementation of compact sources of circularly polarized light.

DOI: 10.1103/PhysRevApplied.17.L021001

### I. INTRODUCTION

The creation of compact devices that can be used to control the state of polarization of emitted light is one of the central problems of nanophotonics. Analogously to spin-polarized current injectors in spintronics [1], compact sources of circularly polarized emission open up the possibility of their further practical application in such rapidly developing fields as quantum technologies for optical manipulation of quantum information and optoelectronics [2,3].

The conventional strategy to achieve circularly polarized emission is to use quarter-wave plates, which are far from being spatially compact. A widely explored route towards implementing compact circularly polarized lasers involves the use of optical or electric spin injection (so-called spin-lasers) [4–12], or optically chiral media. A lot of attention has been devoted to cholesteric liquid crystals [13–19]. However, from a practical and thus application-oriented perspective, all-solid chiral photonic or plasmonic structures, photonic crystals, and metasurfaces are advantageous due to their compatibility with existing, widely

used laser and semiconductor technologies [3,20–28]. The use of photonic crystals and metasurfaces also opens a recently developed nonlinear optical route towards circularly polarized light emission through the generation of third and higher harmonics [29–32]. Note that chiral dielectric microresonators have been extensively explored for controlling light flow and achieving directional lasing output of whispering gallery modes, due to a stronger out-coupling for, e.g., the counterclockwise-propagating mode, rather than for the clockwise-propagating one in a chiral microcavity (e.g., [33]; for an exhaustive review, see [34]).

A straightforward possibility to achieve circularly polarized photoluminescence (PL) in conventional achiral III-V semiconductors is introduced in Refs. [22,23] when a very thin modulated structure with chiral symmetry is formed in the upper layer by partial etching. In such nanostructures, the inequivalence of the right- and left-polarized electromagnetic modes arises due to the general chiral symmetry of the system, and it can be used to create compact circularly polarized light emitters without applying an external magnetic field, and without the need for spin-polarized injection.

Utilizing this approach, circularly polarized PL [23,26,27,35] in full agreement with the theoretical

\*maksimov@issp.ac.ru

calculations [26,27,36], and even lasing under optical pumping [37] were demonstrated in active III-V cavities. Except demonstrations in the THz range [25,38,39], harnessing the concept of fishbone-aperture antennas, lasing under electrical pumping in chiral cavities has remained elusive.

In this Letter, we present this most critical step towards application relevance of the suggested approach, and demonstrate a circularly polarized laser via electric pumping, based on a microcavity with quantum wells (QWs) in the active region and with a chirally modulated upper Bragg mirror.

## II. SAMPLES

Our laser diode (Fig. 1) is based on a microcavity (MC) structure with (Al, Ga)As/AlAs pairs in the top and in the bottom distributed Bragg reflectors (DBRs), four GaAs QWs in an intrinsic one-wavelength-thick cavity ( $\lambda$ -cavity), and a chiral photonic crystal (CPC) slab on the top of the upper cavity mirror.

The sample is grown by molecular beam epitaxy on a (100)-oriented silicon-doped (*n*-doped) GaAs substrate. The full planar cavity consists of 23.5 AlAs/Al<sub>0.20</sub>Ga<sub>0.80</sub>As Bragg pairs in the top DBR, 27 Bragg pairs in the bottom DBR, and 4 GaAs QWs (4 × 7 nm separated by 4-nm-thick Al<sub>0.40</sub>Ga<sub>0.60</sub>As barriers) in an intrinsic Al<sub>0.40</sub>Ga<sub>0.60</sub>As  $\lambda$ -cavity [Fig. 1(a), bottom right]. The 27 AlAs/Al<sub>0.20</sub>Ga<sub>0.80</sub>As Bragg pairs in the bottom DBR are gradually *n*-doped by Si with concentration varying from  $3 \times 10^{18}$  cm<sup>-3</sup> to  $1 \times 10^{18}$  cm<sup>-3</sup> (Si- $\delta$ -dopings at electric field minima); the 23.5 AlAs/Al<sub>0.20</sub>Ga<sub>0.80</sub>As Bragg pairs in the top DBR are gradually *p*-doped by C with concentrations from  $3 \times 10^{18}$  cm<sup>-3</sup> to  $1 \times 10^{18}$  cm<sup>-3</sup> (C- $\delta$ -dopings) and a highly doped topmost mirror ( $1 \times 10^{19}$  cm<sup>-3</sup>) for Ohmic contact.

The individual laser structures are micropillars with  $60 \times 60 \mu\text{m}^2$  base size. A schematic of such a laser MC is depicted in Fig. 1(a). A chiral photonic crystal slab of  $36 \times 36 \mu\text{m}^2$  in size is fabricated in an area confined within a gold circular contact by electron-beam lithography and reactive ion etching of the upper cavity mirror. It represents a square lattice with unit cells consisting of four nanopillars with elongated rectangles in their bases and rotated by  $90^\circ$  to the left or right, relative to one another [Fig. 1(a), top right], similar to those used in optically pumped laser structures [37]. The structure has a broken in-plane mirror symmetry and  $C_4$  point symmetry. It is three-dimensionally chiral, because it does not have planes of mirror symmetry, including the horizontal one, that provides strong optical activity [21]. In our structure, we choose the following geometric parameters: slab thickness (the depth of etching)  $N_{\text{etch}} = 4.75$  Bragg pairs (i.e., the four top Bragg pairs, the next AlAs layer, and half of the Al<sub>0.20</sub>Ga<sub>0.80</sub>As layer of the fifth Bragg pair),

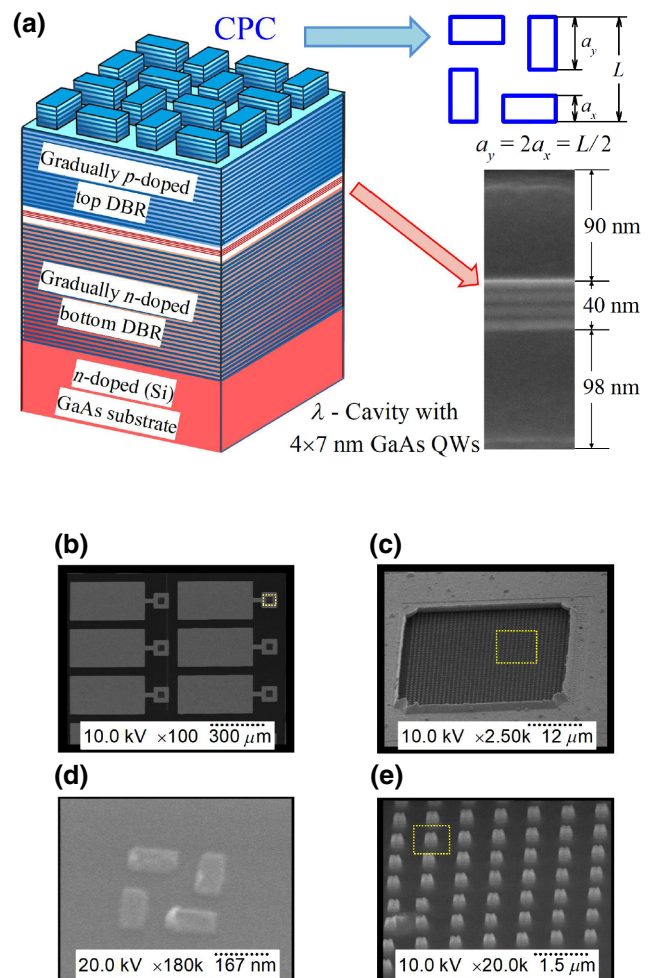


FIG. 1. The schematics of a sample with electrically pumped chiral modulated semiconductor microcavities with circularly polarized laser emission. (a) Part of the laser microcavity with four unit cells of a CPC on the top of the structure (left); top right: relative sizes of the “left” chiral unit cell’s elements (view from above); bottom right: scanning electron microscopy image of  $\lambda$ -cavity (thickness approximately 228 nm) with four GaAs QWs. (b) Part of a sample with several laser structures (view from above). (c) Single laser microcavity with gold contact. (d) Several unit cells of CPC. (e) A single unit cell of CPC, consisting of four rectangular pillars, on the top of the laser microcavity. The contents of yellow dashed rectangles in (b), (c), and (d) are shown magnified in (c), (d), and (e), respectively.

photonic crystal period  $d = 880$  nm, and the feature size  $L$  [Fig. 1(a)] varying from 256 to 280 nm.

## III. EXPERIMENT

A pulsed voltage is applied to each laser of up to approximately 15 V for excitation. Pulse excitation allows us to apply higher voltages without damaging the laser structure. The duration of rectangular excitation pulses is chosen as approximately 1  $\mu\text{s}$  at a repetition frequency of 10 kHz.

The sample is held at temperature  $T \simeq 1.8$  K in an optical cryostat in superfluid He. The emission is collected by a long-working-distance microscope objective, which provides spatial resolution of approximately 1  $\mu\text{m}$ . Using a small aperture allows us to analyze spectra with angle resolution of approximately  $0.5^\circ$  in the direction close to the normal to the sample surface. The emission light is dispersed by a spectrometer and detected by a Si CCD camera. The polarization of the emission is analyzed by a quarter-wave retarder and linear polarizers.

#### IV. RESULTS

Figure 2 shows the set of electroluminescence emission spectra of one such laser structure at different values of excitation pulse current  $J$  flowing through a sample. At low levels of excitation pulse current  $J$  the emission spectra present a rather broad line with half-width of 1 meV [Figs. 2(d) and 2(c)]. Several laser modes appear as the current increases, and a drastic superlinear increase of the emission line intensity is observed [Fig. 2(b) and 2(a)]. This increase is accompanied by a narrowing of the full width at half maximum to values about  $\lesssim 40$   $\mu\text{eV}$  (the resolution of our spectrometer) and angular spatial distributions of about  $1.5^\circ$ – $2^\circ$ .

A typical dependence of the laser emission intensity on excitation pulse current  $J$  is presented in Fig. 3(a). It is seen that the linear dependence of emission intensity  $I \propto J$  at weak currents is superseded by its sharp superlinear ( $I \propto J^{12}$ ) increase upon reaching threshold current values  $J_{\text{th}} \approx 10$  mA.

In Fig. 3(b), shown by filled circles, we plot the degree of circular polarization of the emission  $\rho_c$ , defined as  $\rho_c = (I^+ - I^-)/(I^+ + I^-)$ , where  $I^+$  and  $I^-$  are the emission line intensities in two circular polarizations  $\sigma^+$  and  $\sigma^-$ , respectively. At weak currents (in the regime of spontaneous emission), it only acquires a modest value of  $\rho_c \lesssim 10\%$ . As the lasing threshold is crossed at injection currents of 10 mA,  $\rho_c$  features a sharp increase with the pulsed injection current [Fig. 3(b)].

In order to understand the physical reason for the  $\rho_c$  growth in the lasing regime let us note first of all that the investigated structure has a “weaker” chirality, compared with our previous work on optically pumped lasing in a microcavity with optimized chiral modulated upper Bragg mirror [37]. The calculated  $\rho_c$  in the spontaneous regime in this structure, caused by its  $C_4$  symmetry, is expected to be only 5%–10% maximum (compared with 70%–80% for the optimized structures in Ref. [37]). This agrees with the experimental values below the lasing threshold [see Fig. 3(b)]. The  $\rho_c$  growth with the lasing is caused, we believe, by the nonlinear behavior in the exciton-polariton system.

The important point here is that even in the case of “weak” chirality, the lowered  $C_4$  symmetry of the structure

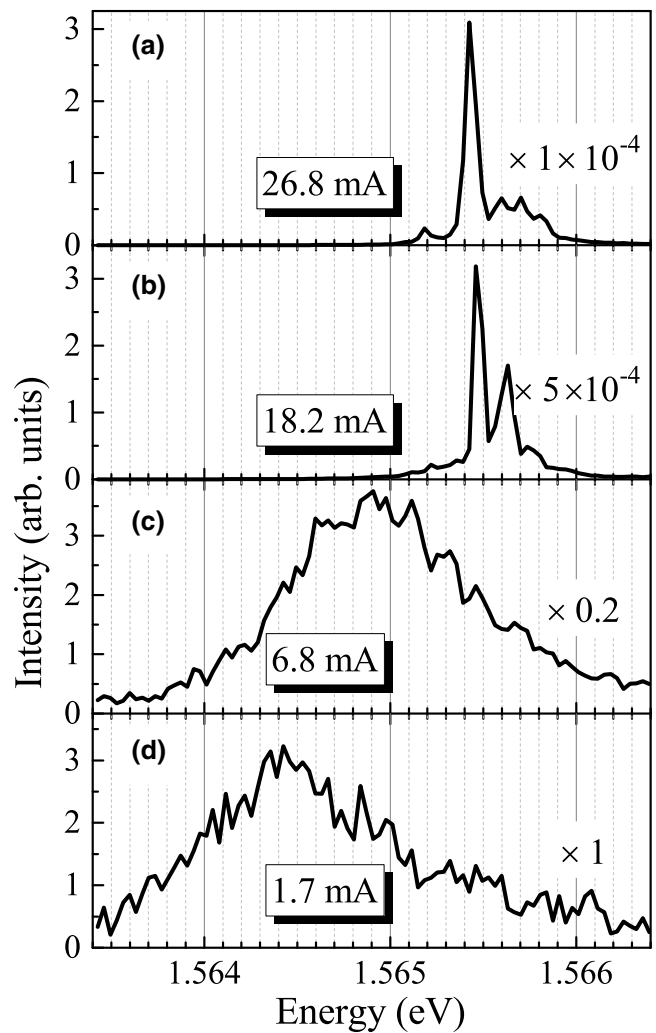


FIG. 2. Electroluminescence emission intensity spectra of a laser structure ( $L = 264$  nm) at different values of excitation pulse current  $J$  at values above (a),(b) and below (c),(d) the threshold current  $J_{\text{th}} \approx 10$  mA.

provides a lower lasing threshold for the major circular polarization mode of the exciton-polariton system in our structure, as was observed in an optically spin-injected vertical-cavity surface-emitting laser [7]. This dictates the overall predominance of this mode above the lasing threshold even if this predominance is weak in the spontaneous regime. In this sense, this effect is analogous to the switching of the planar microcavity polariton system into the circularly polarized state [40,41]. However, there is an important difference: the switching to circularly polarized state is caused here by the earlier transition into the stimulated lasing regime for the predominant mode, whereas in Refs. [40,41] it was due to the multistability switching under resonant pumping.

Strictly speaking, according to this argument, the emission of our  $C_4$  system in the one-mode lasing regime has

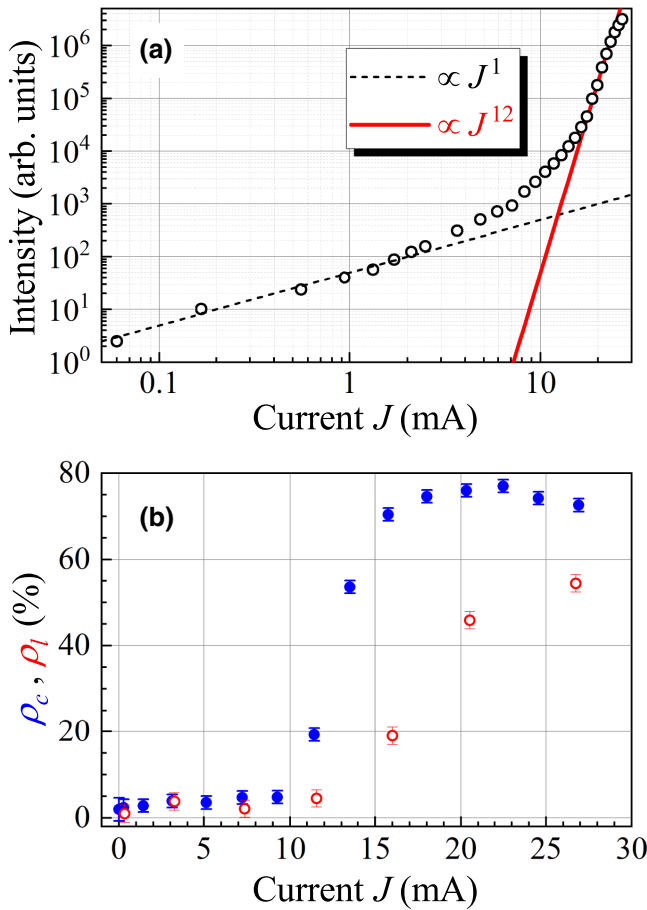


FIG. 3. (a) Emission intensity dependence of the laser structure ( $L = 264$  nm) on excitation pulse current  $J$ . (b) Typical dependencies of the circular  $\rho_c$  (filled circles) and linear  $\rho_l$  (open circles) polarization degree of the emission on the excitation pulse current  $J$  for the same laser structure.

to be close to 100% circularly polarized. In fact, however, in high-quality laser structures, typical values of  $\rho_c$  in the lasing regime reach a plateau around  $\gtrsim 70\%$  [see Fig. 3(b)]. A more detailed study of the polarization at high  $J$  in these structures shows that in the lasing regime the emission features a value of the total elliptic polarization  $\sqrt{\rho_c^2 + \rho_l^2}$  very close to 100% like that in Fig. 3(b) at  $J \approx 2J_{\text{th}}$ . Here  $\rho_l$  is the degree of linear polarization; it is also measured and shown for the same laser structure by open circles in Fig. 3(b). The linear polarization appears most probably due to a lower symmetry of the real structure than  $C_4$ . The possible reasons for the appearance of partial linear polarization of laser generation in such types of structures are structural imperfections from the etching and/or unidirectional crystal strain [37].

Interestingly, we find that the maximum value of the circular polarization degree  $\rho_c$  in some narrow lines (laser modes) can reach values larger than 90% as shown in Fig. 4 as an example.

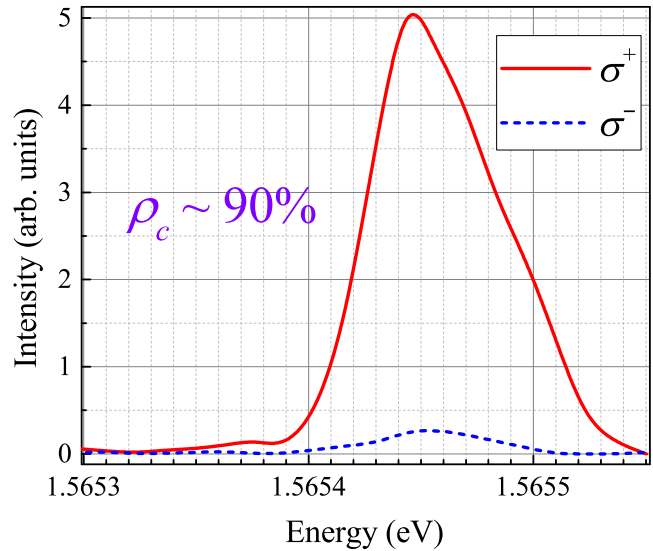


FIG. 4. The emission spectra in the developed lasing regime in  $\sigma^+$  and  $\sigma^-$  circular polarizations of chiral laser structure ( $L = 268$  nm,  $J \approx 25$  mA) with the achieved value  $\rho_c \approx 90\%$ .

Since the polarization character of the laser emission  $\rho_c$  is dictated by the symmetry of the microcavity, the sign of circular polarization of laser emission ( $\sigma^+$  or  $\sigma^-$ ) depends on the handedness of a photonic crystal slab (left- or right-twisted rectangular nanopillars in the unit cell) on the top of the upper DBR. This is verified in Figs. 5(a) and 5(b), where we plot the emission spectrum in  $\sigma^+$  and  $\sigma^-$  circular polarizations after a thresholdlike transition to the lasing

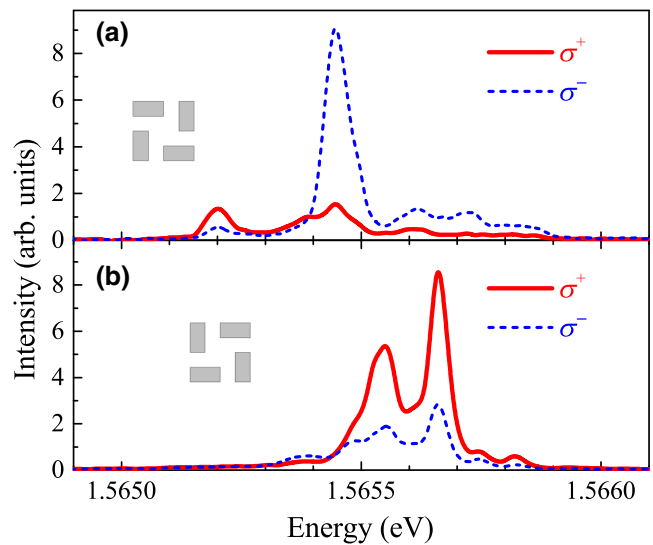


FIG. 5. The emission spectra in the developed lasing regime in  $\sigma^+$  and  $\sigma^-$  circular polarizations of two laser structures with close parameters ( $L = 264$  nm,  $J \approx 27$  mA) but with opposite handedness of the photon crystal on the top of the upper DBR: left (a) and right (b).

regime in two laser microstructures with close parameters and opposite handedness of the photonic crystal (left and right, respectively). Although these two lasers do not show completely identical spectra due to possible structural imperfections, a clear correlation is seen between the circular polarization degree of the most intense laser modes and the handedness of the photonic crystal slab.

## V. CONCLUSIONS

In conclusion, we demonstrate electrically pumped laser emission based on an AlAs/(Al, Ga)As Bragg microcavity with a chirally etched DBR segment, and establish this structure as a compact source of circularly polarized laser emission. Our study verifies that the sign of the polarization (clockwise or counterclockwise) can be set at the stage of manufacture via the symmetry of the chiral photonic crystal mirror. The advantage of using chiral photonic crystal slabs with a large contrast of dielectric permittivity is their giant optical activity that allows one to fabricate a very thin “wave plate” with a thickness of the order of the emitted light wavelength, and integrated in compact laser sources. Adaption of the structure design will allow the implementation of devices operating at room temperature. We anticipate that optimized structures can be operated in the strong coupling regime, promising ultralow thresholds combined with largest polariton nonlinearities [42]. Our success in implementing chiral electro-optical cavities can furthermore be a valuable resource in twisttronics engineering of quantum materials in the strong light-matter coupling regime [3].

## ACKNOWLEDGMENTS

This work is partially supported by the Russian Foundation for Basic Research, Projects No. 19-02-00697 and No. 20-02-00534. C.S. is grateful for support by the German Research Society (DFG) within Project No. SCHN1376-13.1.

- [1] X. Jiang, R. Wang, R. M. Shelby, R. M. Macfarlane, S. R. Bank, J. S. Harris, and S. S. P. Parkin, Highly Spin-Polarized Room-Temperature Tunnel Injector for Semiconductor Spintronics Using MgO(100), *Phys. Rev. Lett.* **94**, 056601 (2005).
- [2] P. Genevet, F. Capasso, F. Aieta, M. Khorasaninejad, and R. Devlin, Recent advances in planar optics: From plasmonic to dielectric metasurfaces, *Optica* **4**, 139 (2017).
- [3] H. Hübener, U. De Giovannini, C. Schäfer, J. Andberger, M. Ruggenthaler, J. Faist, and A. Rubio, Engineering quantum materials with chiral optical cavities, *Nat. Mater.* **20**, 438 (2021).
- [4] H. Ando, T. Sogawa, and H. Gotoh, Photon-spin controlled lasing oscillation in surface-emitting lasers, *Appl. Phys. Lett.* **73**, 566 (1998).

- [5] M. Holub and P. Bhattacharya, Spin-polarized light-emitting diodes and lasers, *J. Phys. D—Appl. Phys.* **40**, R179 (2007).
- [6] H. Fujino, S. Koh, S. Iba, T. Fujimoto, and H. Kawaguchi, Circularly polarized lasing in a (110)-oriented quantum well vertical-cavity surface-emitting laser under optical spin injection, *Appl. Phys. Lett.* **94**, 131108 (2009).
- [7] S. Iba, S. Koh, K. Ikeda, and H. Kawaguchi, Room temperature circularly polarized lasing in an optically spin injected vertical-cavity surface-emitting laser with (110) GaAs quantum wells, *Appl. Phys. Lett.* **98**, 081113 (2011).
- [8] A. A. Qader, Y. Hong, and K. A. Shore, Lasing characteristics of VCSELs subject to circularly polarized optical injection, *J. Lightwave Technol.* **29**, 3804 (2011).
- [9] J.-Y. Chen, T.-M. Wong, C.-W. Chang, C.-Y. Dong, and Y.-F. Chen, Self-polarized spin-nanolasers, *Nat. Nanotechnol.* **9**, 845 (2014).
- [10] A. Elarabi, Y. Yoshioka, M. Tsujimoto, and I. Kakeya, Monolithic Superconducting Emitter of Tunable Circularly Polarized Terahertz Radiation, *Phys. Rev. Appl.* **8**, 064034 (2017).
- [11] M. Lindemann, G. Xu, T. Pusch, R. Michalzik, M. R. Hofmann, I. Žutić, and N. C. Gerhardt, Ultrafast spin-lasers, *Nature* **568**, 212 (2019).
- [12] I. Žutić, G. Xu, M. Lindemann, P. E. Faria Jr, J. Lee, V. Labinac, K. Stojšić, G. M. Sipahi, M. R. Hofmann, and N. C. Gerhardt, Spin-lasers: Spintronics beyond magnetoresistance, *Solid State Commun.* **316–317**, 113949 (2020).
- [13] V. I. Kopp, B. Fan, H. K. M. Vithana, and A. Z. Genack, Low-threshold lasing at the edge of a photonic stop band in cholesteric liquid crystals, *Opt. Lett.* **23**, 1707 (1998).
- [14] V. I. Kopp, Z.-Q. Zhang, and A. Z. Genack, Lasing in chiral photonic structures, *Prog. Quantum Electron.* **27**, 369 (2003).
- [15] Y. Tanaka, H. Takano, and T. Kurokawa, Circular polarization resonator based on cholesteric liquid crystal, *Jpn. J. Appl. Phys.* **43**, 1062 (2004).
- [16] Y. Zhou, Y. Huang, A. Rapaport, M. Bass, and S.-T. Wu, Doubling the optical efficiency of a chiral liquid crystal laser using a reflector, *Appl. Phys. Lett.* **87**, 231107 (2005).
- [17] Y. Zhou, Y. Huang, and S.-T. Wu, Enhancing cholesteric liquid crystal laser performance using a cholesteric reflector, *Opt. Express* **14**, 3906 (2006).
- [18] N. Y. Ha, Y. Ohtsuka, S. M. Jeong, S. Nishimura, G. Suzuki, Y. Takanishi, K. Ishikawa, and H. Takezoe, Fabrication of a simultaneous red-green-blue reflector using single-pitched cholesteric liquid crystals, *Nat. Mater.* **7**, 43 (2008).
- [19] C.-T. Wang and T.-H. Lin, Polarization-tunable chiral nematic liquid crystal lasing, *J. Appl. Phys.* **107**, 123102 (2010).
- [20] P. C. P. Hrudey, B. Szeto, and M. J. Brett, Strong circular Bragg phenomena in self-ordered porous helical nanorod arrays of Alq<sub>3</sub>, *Appl. Phys. Lett.* **88**, 251106 (2006).
- [21] D.-H. Kwon, P. L. Werner, and D. H. Werner, Optical planar chiral metamaterial designs for strong circular dichroism and polarization rotation, *Opt. Express* **16**, 11802 (2008).
- [22] K. Konishi, B. Bai, X. Meng, P. Karvinen, J. Turunen, Y. P. Svirko, and M. Kuwata-Gonokami, Observation of extraordinary optical activity in planar chiral photonic crystals, *Opt. Express* **16**, 7189 (2008).

- [23] K. Konishi, M. Nomura, N. Kumagai, S. Iwamoto, Y. Arakawa, and M. Kuwata-Gonokami, Circularly Polarized Light Emission from Semiconductor Planar Chiral Nanostructures, *Phys. Rev. Lett.* **106**, 057402 (2011).
- [24] N. Shitrit, I. Yulevich, E. Maguid, D. Ozeri, D. Veksler, V. Kleiner, and E. Hasman, Spin-optical metamaterial route to spin-controlled photonics, *Science* **340**, 724 (2013).
- [25] P. Rauter, J. Lin, P. Genevet, S. P. Khanna, M. Lachab, A. Giles Davies, E. H. Linfield, and F. Capasso, Electrically pumped semiconductor laser with monolithic control of circular polarization, *Proc. Natl. Acad. Sci. USA* **111**, E5623 (2014).
- [26] A. A. Maksimov, I. I. Tartakovskii, E. V. Filatov, S. V. Lobanov, N. A. Gippius, S. G. Tikhodeev, C. Schneider, M. Kamp, S. Maier, S. Höfling, and V. D. Kulakovskii, Circularly polarized light emission from chiral spatially-structured planar semiconductor microcavities, *Phys. Rev. B* **89**, 045316 (2014).
- [27] S. V. Lobanov, S. G. Tikhodeev, N. A. Gippius, A. A. Maksimov, E. V. Filatov, I. I. Tartakovskii, V. D. Kulakovskii, T. Weiss, C. Schneider, J. Geßler, M. Kamp, and S. Höfling, Controlling circular polarization of light emitted by quantum dots using chiral photonic crystal slabs, *Phys. Rev. B* **92**, 205309 (2015).
- [28] W.-C. Liao, S.-W. Liao, K.-J. Chen, Y.-H. Hsiao, S.-W. Chang, H.-C. Kuo, and M.-H. Shih, Optimized spiral metal-gallium-nitride nanowire cavity for ultra-high circular dichroism ultraviolet lasing at room temperature, *Sci. Rep.* **6**, 26578 (2016).
- [29] N. M. Litchinitser, Nonlinear optics in metamaterials, *Adv. Phys.-X* **3**, 1367628 (2018).
- [30] L. Carletti, S. S. Kruk, A. A. Bogdanov, C. De Angelis, and Y. Kivshar, High-harmonic generation at the nanoscale boosted by bound states in the continuum, *Phys. Rev. Res.* **1**, 023016 (2019).
- [31] G. Ban, C. Gong, C. Zhou, S. Li, R. Barille, X. Liu, and Y. Wang, Fano-resonant silicon photonic crystal slab for efficient third-harmonic generation, *Opt. Lett.* **44**, 126 (2019).
- [32] K. Konishi, D. Akai, Y. Mita, M. Ishida, J. Yumoto, and M. Kuwata-Gonokami, Circularly polarized vacuum ultraviolet coherent light generation using a square lattice photonic crystal nanomembrane, *Optica* **7**, 855 (2020).
- [33] B. Peng, S. K. Özdemir, M. Liertzer, W. Chen, J. Kramer, H. Yilmaz, J. Wiersig, S. Rotter, and L. Yang, Chiral modes and directional lasing at exceptional points, *Proc. Natl. Acad. Sci. USA* **113**, 6845 (2016).
- [34] H. Cao and J. Wiersig, Dielectric microcavities: Model systems for wave chaos and non-Hermitian physics, *Rev. Mod. Phys.* **87**, 61 (2015).
- [35] A. A. Maksimov, A. B. Peshcherenko, E. V. Filatov, I. I. Tartakovskii, V. D. Kulakovskii, S. G. Tikhodeev, S. V. Lobanov, C. Schneider, and S. Höfling, Polarization, spectral, and spatial emission characteristics of chiral semiconductor nanostructures, *JETP Lett.* **106**, 643 (2017).
- [36] S. V. Lobanov, T. Weiss, N. A. Gippius, S. G. Tikhodeev, V. D. Kulakovskii, K. Konishi, and M. Kuwata-Gonokami, Polarization control of quantum dot emission by chiral photonic crystal slabs, *Opt. Lett.* **40**, 1528 (2015).
- [37] A. A. Demenev, V. D. Kulakovskii, C. Schneider, S. Brodbeck, M. Kamp, S. Höfling, S. V. Lobanov, T. Weiss, N. A. Gippius, and S. G. Tikhodeev, Circularly polarized lasing in chiral modulated semiconductor microcavity with GaAs quantum wells, *Appl. Phys. Lett.* **109**, 171106 (2016).
- [38] G. Z. Liang, Y. Q. Zeng, X. N. Hu, H. Yu, H. K. Liang, Y. Zhang, L. H. Li, A. G. Davies, E. H. Linfield, and Q. J. Wang, Monolithic semiconductor lasers with dynamically tunable linear-to-circular polarization, *ACS Photonics* **4**, 517 (2017).
- [39] L. Y. Xu, D. G. Chen, C. A. Curwen, M. Memarian, J. L. Reno, T. Itoh, and B. S. Williams, Metasurface quantum-cascade laser with electrically switchable polarization, *Optica* **4**, 468 (2017).
- [40] S. S. Gavrilov, A. V. Sekretenko, S. I. Novikov, C. Schneider, S. Höfling, M. Kamp, A. Forchel, and V. D. Kulakovskii, Polariton multistability and fast linear-to-circular polarization conversion in planar microcavities with lowered symmetry, *Appl. Phys. Lett.* **102**, 011104 (2013).
- [41] S. S. Gavrilov, A. S. Brichkin, S. I. Novikov, S. Höfling, C. Schneider, M. Kamp, A. Forchel, and V. D. Kulakovskii, Nonlinear route to intrinsic Josephson oscillations in spinor cavity-polariton condensates, *Phys. Rev. B* **90**, 235309 (2014).
- [42] C. Schneider, A. Rahimi-Iman, N. Y. Kim, J. Fischer, I. G. Savenko, M. Amthor, M. Lermer, A. Wolf, L. Worschech, V. D. Kulakovskii, I. A. Shelykh, M. Kamp, S. Reitzenstein, A. Forchel, Y. Yamamoto, and S. Höfling, An electrically pumped polariton laser, *Nature* **497**, 348 (2013).